1. Executive Summary

Ankle-foot orthotics (AFOs) are widely used supportive devices that give people with limited ankle and foot control greater support and mobility. Unfortunately, these devices are limited by their inability to provide dynamic properties – namely stiffness – to allow the user a wide range of motion. In this report, we propose a variable stiffness AFO that continuously adjusts the stiffness to maintain the user's ankle in a safe range. We further design and develop a prototype system that demonstrates the validity of the proposed device by operating effectively under scaled conditions. The validation comes from experimental results on the prototype system that are compared with simulations of our developed model that show good adherence between the two. Finally, we analyze the ethical, legal, environmental, and financial implications of this project, with a focus on the considerations that are important for continued development.

2. Introduction

Individuals with neurological or musculoskeletal disorders or injuries often have limited control or weakness in their ankles, and as a result are unable to walk without their feet dropping and dragging [1]. This "foot drop" can lead to pain and injury from hyperextension or even the inability to walk altogether; therefore, these individuals often rely on mobility aids, such as a wheelchair, or surgical procedures, which may be costly, dangerous, or ineffective. Another solution, however, is to wear a brace. These braces, known as ankle-foot orthotics (AFOs), add support to the ankle to prevent extension outside a safe range of motion, which may eliminate the need for mobility aids or surgical procedures. AFOs are the most commonly used orthosis in the United States and are used for a variety of purposes, but primarily work to compensate for lower limb weakness and control foot drop [2].

One of the current problems with modern day AFOs is that they require varying mechanical properties – namely stiffness – to function properly over a typical range of physical activities. For example, running requires a stiffer orthotic than walking due to the increased forces and change in ankle rotation. For this reason, Fabtech Systems has designed an AFO which has five different composite "beams" that can be interchanged depending on the user's activity. Each beam has a different thickness, and therefore bending stiffness, which allows users to choose a stiffness to match their activity level. However, this solution creates a drawback where the user needs to manually switch between beams when changing their activity level. This can be both inconvenient and time consuming and also requires users to always carry their range of bars and the necessary tools to change them out. There then exists a need to either streamline or even automate this process.

3. Design Approach

In order to address the drawbacks with existing AFOs, we aim to create a single bar design that automatically detects the user's change in physical activity and adjust its stiffness accordingly. This design requires us to develop a method of stiffness variation, activity detection, and mechanical actuation. Therefore, we employ the use of electro-mechanical components which are often absent in existing AFOs. Other groups have created similar designs; however, other drawbacks are often created in development. Some designs are bulky and heavy while others do not have enough variation in stiffness. Our goal is to then create a proof-of-concept prototype to demonstrate the feasibility of our design concept and then optimize stiffness variation and reduce overall size for implementation in an orthotic.

For our approach, we started with the design geometry of Fabtech Systems' AFO to determine the approximate size and general form of our design, and planned to keep our device constrained between the original AFO's fastening points located at the calf and ankle. First, in order to consolidate our device into a single bar design, we studied multiple design techniques before settling on our final design concept which makes use of the bending mechanics of cantilever beams. From our research, we found that the

bending stiffness of a cantilever beam is dependent on the length of the beam. This way, we could increase or decrease stiffness by varying the effective length of a single bar. Next, to detect the user's activity level and adjust the effective length, we needed a sensor at the ankle to read the ankle rotation in real-time, a microcontroller to run our detection and controller programs, and an actuator to mechanically move our system.

With limited time and resources to brainstorm, develop, and test our design concept, we decided to design a bench-top device instead of an orthotic that could actually be attached to a person's leg. This way, we could perform controlled bench testing to determine the efficacy of our proof-of-concept design without needing to manufacture the parts needed to fit it on a person. With this direction, we were also able to eliminate the need to account for the complexities of the human gait and scale down the forces for our testing procedures. This then lessened the cost and difficulty of designing and fabricating parts to handle the larger forces experienced while walking.

4. Functional Requirements

Table 1: Desired Specifications

Specification	Desired Value
Rise Time	6 s
Settling Time	15 s
Overshoot	10 %
Weight	5-6 lbs
Ankle Angle Range	5 deg to -5 deg
Maximum Length	250 mm
Stiffness Range (Prototype)	0.576 - 2.667 kN/m

Table 1 details our functional specifications. These values have undergone refinement throughout the design process of the controller. The rise time can be fairly large, but ideally the "rising" would only occur while the foot is in the air in order to conserve power. We determined that our rise time should be about six seconds, which should result in an increase in stiffness significantly before the ankle bends beyond the safe angle range. The settling time is less important than the rise time or the overshoot, but the stiffness should stop changing within a few seconds of rising to the necessary value. Because of this, we determined that a 15 second settling time would be reasonable.

The overshoot is important in order to avoid too stiff of a beam that would disrupt the user's stride. A fairly low overshoot, of 10% or less, is ideal. The weight of the final design is important for similar reasons. While it will not be critical in our prototype, the weight of the design should be similar to the weight of Fabtech's current orthotic, otherwise the device will become cumbersome and users may opt to deal with the inconvenience of multiple bars. Ideally the weight of the final product should be, at maximum, 120% of Fabtech's product, allowing the device to weigh 5 to 6 pounds. The ankle angle range of ± 5 degrees will provide a natural stride. Our stiffness range will also be slightly more extensive than Fabtech's design in order to provide more comfort to the user and to accommodate a more diverse user base. Also to keep the device wearable for the user, the max length of the cantilever beam was set to 250 mm.

5. Theoretical Models and Simulations

5.1 Mechanical Design

This design makes use of cantilever beam mechanics by adjusting the effective length of our beam shown in Figure 1. As seen in Equation 1, the bending stiffness, $K_{bending}$, of a cantilever beam is inversely proportional to the length, L, of the beam squared, meaning that as L decreases, the bending stiffness of our beam increases which also decreases the deflection of the beam. L can then be controlled to accommodate different physical activities. P is the applied force at the end of the cantilever beam which represents the force produced at the top fastening point when stepping, E is the modulus of elasticity of the material, and I is the second moment of area which can be adjusted by changing the cross-sectional area of our beam.

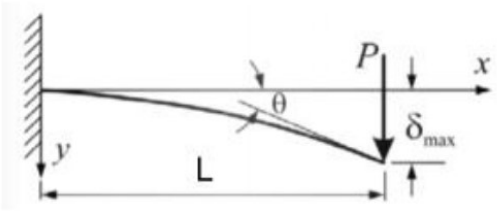

Figure 1: Cantilever Beam

$$K_{bending} = \frac{2EI}{L^2} \tag{1}$$

A commercial product rough sketch for this design is shown in Figure 2. Just as with Fabtech's design, the device will be anchored to the leg at locations near the calf and ankle. There is a cantilever beam that runs from the bottom anchor point upwards. A roller piece can then slide parallel along the length of the cantilever beam to alter its effective length, increasing or decreasing stiffness as needed. A DC motor is used to spin a linear screw that produces the translation motion of the carriage. Additionally, since deflection is not linear in relation to length, for our controller, we must linearize our stiffnesses around specific effective lengths. Figure 3 shows the bench top testing setup for this design and is what was manufactured and tested for this capstone project.

Again, Figure 2 is a very simplistic representation of how our prototype, Figure 3, would transfer over to Fabtech's design. This whole device would only be anchored in two places, yet it would still accomplish the same goal. This prototype was made to simulate the motion of a person as they walk or run. Instead of having the foot and leg creating an angle at the ankle, this model uses a hinge connected to a fixed base, allowing the system to pivot and bend, simulating real walking motion/angle.

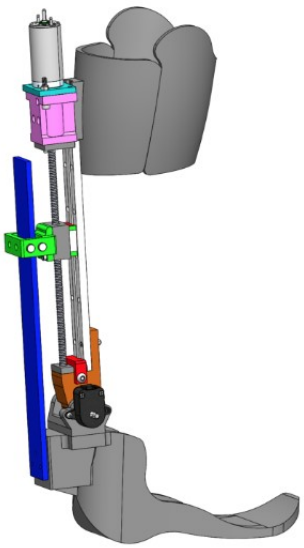

Figure 2: Mock Commercial Product

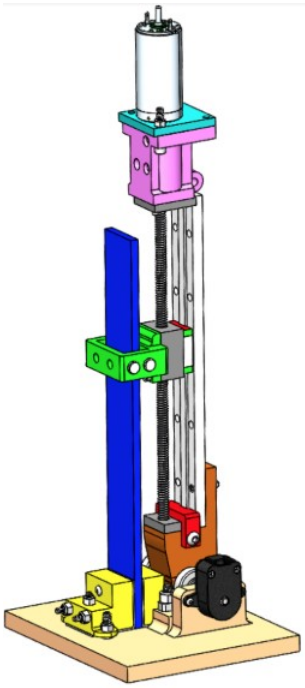

Figure 3: Bench Top Test Setup, The Prototype

This prototype gives exciting insight on how a wearable device would react in certain situations and allow for testing without putting a person in harm's way. The goal of testing this prototype is to study our control system's dynamics. It is critical to know and understand the characteristics of a device well before it is ever tested by a human. While testing, we are confirming that the device is moving the carriage to the correct location, at an appropriate speed for a given amount of force being applied. Along with this, we are also monitoring the amount of current that is being sent to the motor in order to see if the power draw is too much and to see if a different gearbox should be used.

Once we verify that the prototype's control system is working as intended, it is only a matter of changing hardware to adapt it for user testing. The testing for this prototype is directly transferable to the commercial product as both are trying to achieve the same goal. Of course, all of the materials of the structure would have to be revised, but that is well enough understood in classical mechanics that it will not be too hard to implicate it. We would also have to refine our device's power distribution, since currently, a large amplifier is being used to power the motor, but again this is not too difficult to change for future prototypes.

When the prototype was first being designed there were a few key specifications that needed to be considered. This includes what material each component would be made of, what the overall force this prototype would be experiencing, and the overall size of it. Each one of these, along with many more, were key in the design of the final product.

Due to the challenge of manufacturing a cantilever beam that would be able to withstand the forces of regular human walking, the stiffness and strength of the beam were scaled down. This choice was made partially due to the fact that we were not going to be able to manufacture and test a carbon fiber composite beam due to the circumstances of the global pandemic closing down the university. In the model, a beam made of nylon with MDS fill, which was found to have very favorable material properties in terms of flexibility, was used. Unlike common metals such as aluminum and steel, this material is very capable of flexing without failing while still having a large amount of strength. This made this material an excellent choice for our devices as both of these criteria are crucial to the proper functionality of the device.

Using a novel Matlab script, shown in APPENDIX_D_Cantilever_material_Selection.m, different materials, with their relevant material properties, were tested via trial and error methods for the selection of the cantilever beam. While testing a material, the team adjusted the geometric size of the material, namely the width, thickness, and operational length, and analyzed how it would operate under a load defined by the max angle it would oscillate at. This program used simple bending mechanics equations to solve for many important variables. The script would display the force needed to cause this angle and whether or not that force would be safe using the factor of safety of each material's yield stress. It also printed out the upper and lower bounds of stiffness the material would deliver. In the end, the Nylon with MDS was chosen with a geometry of 1.5" wide, 0.25" thick, and an operational length between 150 mm and 250 mm. With this geometry, in the worst case scenario, meaning at the shortest length and pulling with a force that would cause an angle of 20 degrees (well above the normal operational range), the factor of safety of the cantilever beam was 1.54.

Another large consideration that had to be made was the choice of motor that would be used. Using the equations for a mechanical power screw from [3], Equation 2 was used to find how much torque would be required to turn the lead screw, with L is the lead, f is the coefficient of friction of the screw, d_m, is the average diameter of the lead screw, and F is the vertical component of force acting on the lead screw from the carriage.

$$T_R = \frac{(Fd_m/2)((L + \pi f d_m sec(\alpha))}{(\pi d_m - fLsec(\alpha))} \tag{2}$$

Using another original Matlab script, shown in APPENDIX_D_Lead_Screw_Torque_Analysis.m and using a few of the constants used in equation 2, the

overall torque required to turn the lead screw was only 21.35 mN-m. This was well within the range of both of the motors capacity and were used to test this prototype. These motors are a Maxon DC motor and the Pittman DC motor and each of these motor specs sheets can be found in APPENDIX A.

5.2 Electrical Design

In order to facilitate ease of prototyping, numerous electrical components were chosen that had superior performance than what was needed, but had relatively simple operability. One such component was the amplifier used, which was connected to a 110 AC wall outlet and could provide an arbitrarily large current with up to a 48 V signal. For perspective, the motor we chose only required a maximum of 4.9 Amps and a maximum of a 32 V signal, but rarely used more than 3 Amps during operation. The amplifier had many beneficial features, such as an emergency power cutoff, low heat generation, and overcurrent protection.

We also chose a processor that had superior performance than what was required to take advantage of the versatility and built in functionality it provided to increase our speed of development. We chose a myRio device with a 667 MHz dual core Xilinx Z-7010 processor and 512 MB of memory (Appendix B). The myRio device was familiar to us and had plenty of versatility to allow for testing and troubleshooting. The processing speed was far above what our code required, and the total memory was much larger than the 55 kB we used. This allowed us to add and remove pieces of code without worry that our controller would be unable to perform. Furthermore, the myRio device also had a built in DAC, UART processing code, and timer, which further reduced the development time of the prototype code. These features proved very useful and greatly enhanced the speed at which we could develop our prototype, but will need to be individually addressed in the commercial product due to the two important factors: size, and power requirements. The myRio consumes up to 14 W of power and idles at 2.6 W, which is far more than can be supported by batteries housed on the user's leg–our estimates point to about 0.1-0.2 W as the processor power draw that can be supported. The myRio is also far too bulky to fit on a person's leg, with a height and width of 5.4" and 3.4". In the prototyping process, we used a digital LCD and keyboard that connected to the processor through a UART connection, to troubleshoot the code. The embedded UART processing code and dual core processor made this simple to do. The LCD allowed us to analyze the response of the controller and the effectiveness of the peak finding code in real time. The wiring of the prototype system can be found in APPENDIX B - Wiring_Diagram.

To measure the angle of the prototype system and the position of the carriage, two encoders were used. The first encoder (see APPENDIX B - Encoder_$\times$ E5_datasheet), which was used to determine the prototype angle, had a 0.18 deg resolution and typically measured angles within a 15 deg range, this yields a resolution error of approximately 2%, which determined was acceptable given the system's relative tolerance to errors. The second encoder, on the motor, had the same resolution and was used to calculate the position of the carriage, given the gearing of the motor and carriage, the error caused by this encoder was practically negligible.

5.3 Controls

The control system that governs the prototype was built with a peak finding code at its core. In order to calculate the angle of the prototype–the angle of the foot to shin–the quasi continuous encoder data had to be processed such that only the peak values were considered. This allowed the control loop to use the total ankle flexion. As can be seen in Figure 4, where the code is tested with a continuous sinusoid with added noise, the maximum and minimum angle can be taken from the angle data and processed into an absolute signal that can be fed into the control loop. The noise in this case was up to 3% of the sinusoid's amplitude.

The control law was developed to be versatile and robust, with a relatively large settling time and low overshoot. For ease of design and strength of performance, a PIDF controller was used. This controller was easily tuned and able to accommodate a

wide variety of unknown parameters, such as damping, stiffness, transient forces, etc. as can be seen in the results section. Numerous other controllers were experimented with including a lead controller, and cascade PIDF, but neither were found to have significantly superior performance to warrant their continued pursuit.

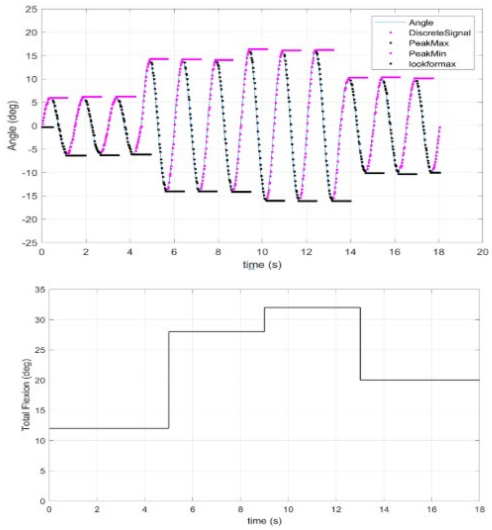

Figure 4: Top) Peak finding analysis with sinusoidal signal and added noise. Bottom) Resulting total flexion signal sent to controller.

As can be seen in Figure 5, the control loop has a fairly typical modular structure, similar to a position control system, with the notable exception of the last three blocks. These blocks come from the linearization of the model around an operating point. For our purposes, we set this point to be the "walking gait", or the average state of applied load, stiffness, and effective length. The following equations can be used to calculate the stiffness of the beam from the effective length (Equation 3) and the predicted flexion angle from the beam stiffness and applied force (Equation 4).

$$K_{bending} = \frac{2EI}{L^2}$$
$$dK = \frac{\delta}{\delta L}\frac{2EI}{L^2}dL$$
$$dK = \frac{-4EI}{L_0^3}dL \tag{3}$$

$$\theta = \frac{f}{K}$$
$$d\theta = \frac{\delta}{\delta K}\frac{f}{K}dK + \frac{\delta}{\delta f}\frac{f}{K}df$$
$$d\theta = \frac{-f_0}{K_0^2}dK + \frac{1}{K_0}df \tag{4}$$

In equations 3 and 4, the 'naught' values represent the operation point value. The linearization means that as the effective length and the disturbance force are farther from the operating point, the model will predict behavior that is farther from the actual behavior. In order to validate the linearization of our plant model, and to confirm that a single set point would provide adequate accuracy, a simulation was completed using SIMULINK by Mathworks, which are detailed in the following section.

5.4 Simulation Results

Our linearized controller design was then tested in SIMULINK to evaluate performance and compare against a non-linearized model. Figures 6-8 show the results of our linear (L) vs non-linear (NL) simulation.

Figure 6 shows the changing effective length of our cantilever beam as varying perpendicular forces are applied. As expected, as the required effective length moves farther from the linearized set point of 200 mm, the NL model (orange) deviates farther from the L model (blue). This can be seen where both models are nearly identical between times 25 - 40 seconds while there is a roughly 30 mm deviation at 40 - 75 seconds.

The effects of the difference in effective length on ankle rotation can be seen in Figure 7. The applied

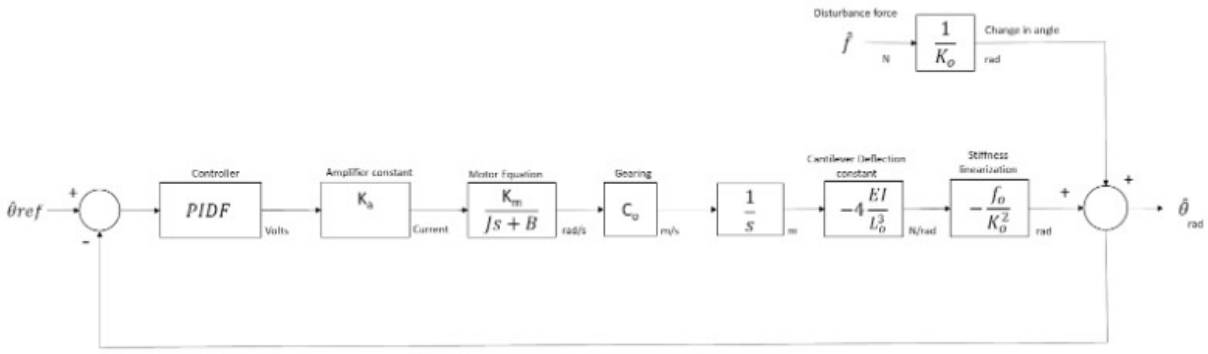

Figure 5: The block diagram for the AFO system.

"Force Angle" (dashed, purple) represents the angle that a specified force would produce at an effective length of 200 mm. Our models were tested for force angles between 5 - 20 degrees, similar to what we would expect from a normal gait. From our plot, we see that the deviations result in different overshoot amounts and settling times; however, both models still remain close together and there are no extreme differences that would raise concern.

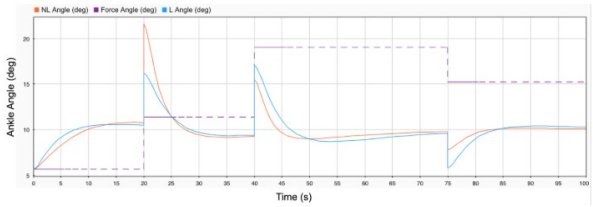

Figure 7: Ankle Angle vs Time Simulation

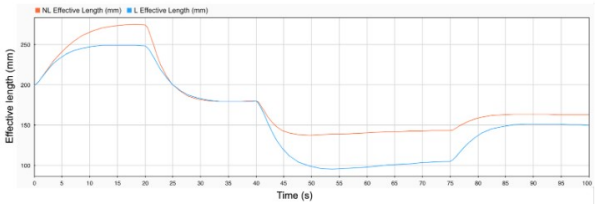

Figure 6: Effective Length vs Time Simulation

The output current supplied to our motor is shown in Figure 8 below. With a set limit of 5.0 amps, we see that in our expected range of force angles, our current model never exceeds our limit. Overall, both L and NL models remain close together and there are no extreme differences.

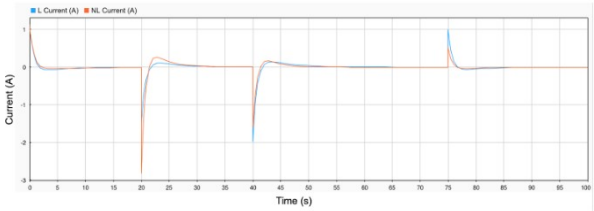

Figure 8: Current vs Time Simulation

6. Prototype

The main structure of the device was manufactured using simple manufacturing at the heart of it. Again, due to the circumstances, manufacturing by machining was out of the question. The team debated on using simpler metal manufacturing including drilling and tapping, and between 3D printing all the parts. In the end, 3D printing ended up being the decision the team went with due to its pure simplicity and lack of headaches. Unfortunately since no one had a 3D printer or knew someone with it, we had to outsource it to a local company who would do it for us. All of the 3D prints have a hexagonal infill and any non-load bearing parts had a 30% infill, while those who were load bearing were 60% infill. In Figure 3, the parts that were 3D printed were the yellow, orange, red, green, magenta, light orange, and teal colored parts. Also not shown is one other 3D printed part that was the adaptor plate for the Pittman motor, it replaces the teal part. All together there were nine different 3D printed parts. Figure 9 shows the CAD model with the major components named for ease of use during the remaining of this report.

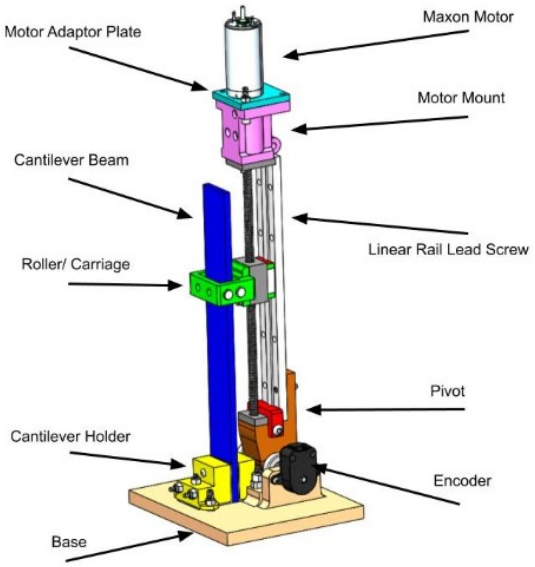

Figure 9: Naming Convention for Prototype

The next major piece of the design is the linear rail lead screw. At first the team was planning on manufacturing our own, but quickly found out this might not be a good idea. In order for the design to work properly and not bind up, extremely tight tolerances would have had to be held.

The would simply would not be possible with the heavy 3D printing manufacturing that was going to be used. Instead, the team decided to change tactics and try to purchase a unit that would have both a linear bearing rail, and a lead screw in one assembly. These types of units are most common in CNC controlled machines such as small mills or in 3D printers, and Figure 10 shows the linear rail lead screw used but the motor was replaced.

Figure 10: FUYU Linear Rail Lead Screw

Next, observing at the roller / Carriage, shown in Figure 11, this part is responsible for pushing and pulling the cantilever beam. Looking closely, there are two clevis pins that were used to enclose the can-

tilever beam. These pins were used because of their circular profile which allows for easy motion of the cantilever as it bends. On that note, as the beam bends, there is translational motion between the pins and the beam, but since the cantilever beam is made of nylon with MDS, the MDS has another incredible feature of having an extremely low coefficient of friction. This allows this translation to occur without the need of a bearing for the pins to roll; it will simply slide across the surface of the pins without too much friction.

The overall goal of this prototype was to confirm that the device would be able to detect a change in force that was being applied to the system. To do this, the angle of the system would be measured and could be used to derive the force that was being applied. An incremental quadrature encoder was used to measure this angle as it pivoted on the base shown in Figure 12.

As the device was pivoted back and forth on the axis of the two bearing sleeves, the screw, that is fixed to the orange part, would turn the incremental encoder. This information would be sent back to the myRio for further analysis and instruction for the system.

A part that was added rather late in the process is the red 3D printed part shown in Figure 13. While designing this prototype, the team got worried about how the orange pivot 3D printed part would handle the stress as it before was only attached with two small screws in the back. The red 3D printed part was added to help distribute this high stress that would have most likely caused the pivot part to fail right at the 90 degree inner corner as its a major stress concentrator.

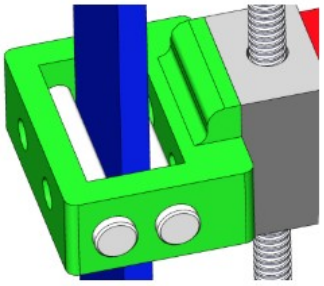

Figure 11: Close-up on Roller and Carriage

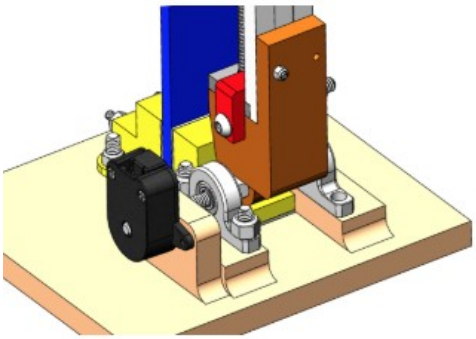

Figure 12: Pivot Angle Measuring

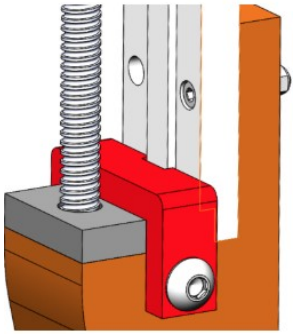

Figure 13: Close Look at the Pivot Attachment

7. Results

The actual prototype adhered well to the design, deviating only with surface finish and a few modified dimensions to facilitate assembly. After the assembly, tests were done on each individual section to confirm that they would work independently. Once it was confirmed that all the individual sections worked, the device was tested all assembled to determine the

accuracy of the initial simulations and models. The following results were taken from a test, in which a force was applied to the motor mount that varied from 10 N to 20 N to 5 N, holding each value for 15 seconds (a plot can be seen in APPENDIX D Applied Force). In Figure 14, the peak finding code is tested based on a varying applied load and a reference angle of 5 deg. The data is quite noisy, so an averaging scheme was set up on the past 500 ms of data to decrease this noise without affecting the overall performance. The averaging effectively eliminated the angle spikes in the data and greatly smoothed it. It's worth noting here that the noise in this data required the implementation of a conditionality that only allowed action on error signals above 20% of the reference angle, else the carriage would constantly move despite a relatively constant flexion angle.

The actual and simulated effective length response was also analyzed, seen in Figure 15. In this analysis, the setpoint length of the beam is 100 mm, which is why the simulated length starts at 100 mm as opposed to 0 mm for the actual effective length.

Finally, the angle response of the entire system was tested against the linearized predicted response, seen in Figure 16. The actual angle exhibits a choppy response, which is a result of the period of oscillation– typically 1-1.5 sec–during which the peak is held constant.

A video of the prototype operating can be found in Appendix F Final Testing.

8. Discussion

8.1 Theoretical vs. Measured

The peak finding algorithm in the final design functions properly, but has significantly more noise than the original peak finding MATLAB script (as can be seen by comparing Figures 4 and 14). This noise is to be expected, however, because the final design was built with robustness in mind. The final peak finding algorithm detects peaks more reliably than the MATLAB script, but also tends to detect false peaks. Ultimately, detecting the true peaks is most crucial because the data from the ankle encoder will never be a perfect sine wave. This robustness, combined with the aforementioned averaging scheme, means that the angle data sent to the encoder will be both accurate and relatively smooth.

In Figure 15, we see that for a given change in measured angle, the actual and simulated beam lengths are very similar. When compared to the difference between the effective lengths of the linear versus nonlinear model (Figure 6), the discrepancy between the actual device and the linear model (Figure 15) is not concerning. This means that for the measured angle data, the control loop is responding as intended. The effectiveness of the controller is corroborated by Figure 17, which shows that the actual angle response to given forces closely follows what we expect from our simulation. Despite the noise in our collected data and the discrete nature of our controller, we see that our control loop can effectively change the stiffness of a cantilever beam in order to maintain a set deflection angle regardless of applied force. Furthermore, the actual device response generally maintains the functional specifications set in the system's design, such as the 15 second settling time.

It is worth noting that there was a non-negligible amount of human error in these tests due to their setup and execution. The transitions between applied forces occurred within $\pm$ 2 s of the desired time, and the applied forces had errors of $\pm$ 3 N.

8.2 Risk and Liability

The factors of safety on each part of the device must be high enough to not only avoid failure, to ensure user safety. Having moving parts near the human body poses some risk, no matter what precautions are taken. This risk makes us liable for injuries caused by the device, and in order to avoid being sued, we must design the device with the users' safety as our top priority. It is also noteworthy that the device has limitations in its range of stiffnesses. The user must be aware that the device is rated for the running speed and forces of the average person, and that it will not be stiff enough to enable them to run competitively. Running at such speeds may result in physical failure

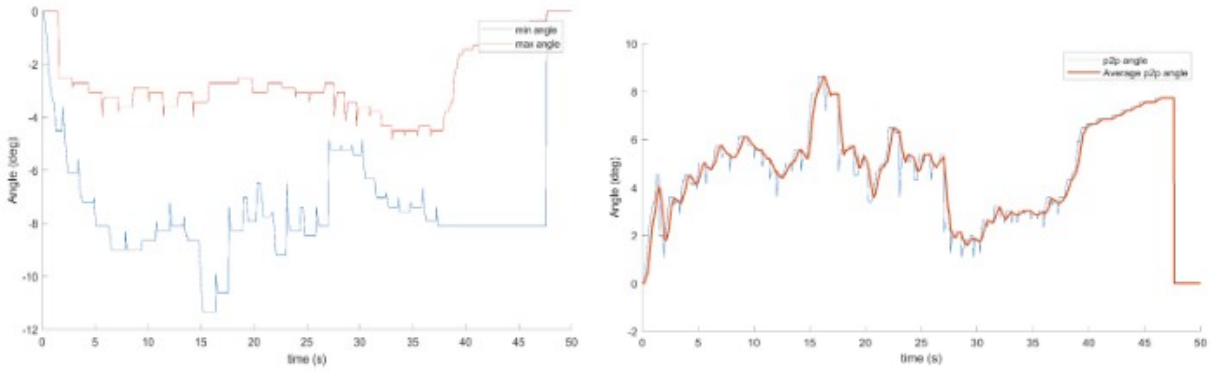

Figure 14: Left) Peak finding data with actual encoder signal. Right) Resulting total flexion signal sent to controller, with and without averaging.

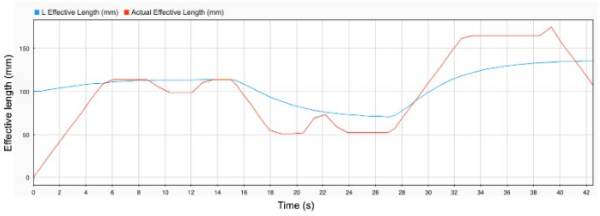

Figure 15: The actual position of the carriage (effective length of the beam) and the linearized prediction of the carriage position.

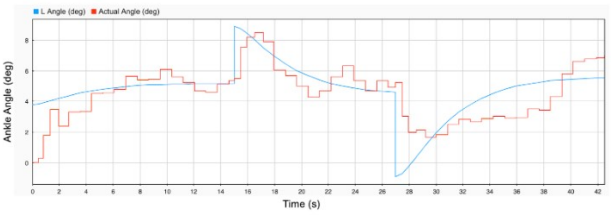

Figure 16: The actual and predicted angle of the AFO in response to varying applied forces.

of the device. Due to this, there must be clear, obvious warnings included with the product in order for the users to protect themselves, and for us to avoid legal liability.

Factors of safety protect against physical failure, but there may also be issues if the response time is too slow. If a user begins to sprint, the device will require a few strides to detect to extreme change and adjust the stiffness accordingly. Too low of beam stiffness could result in part failure or worse, as it could result in further damage to the user's already weak ankles. On the other hand, too fast of a response may lead to controller instability. This instability could also lead to damage, and so we must be careful with our controller design in order to avoid too slow or too fast of a reaction.

Aside from injuries related to device failure, the user may suffer from altered gait due to orthotic. Our device is designed to allow a range of $\pm$ 10 degrees in the ankle, but many people walk with a range of $\pm$ 15 and run with a range of $\pm$ 30 degrees [4]. Research by Elizabeth Russell has indicated that this restricted range of motion, which is caused by most ankle-foot orthotics, does not significantly alter the legs' biomechanics [5], and others indicate that it actually improves the user's gait [1]. However, we would likely need to do our own testing on our device specifically, as a severely altered gait could affect the user in other areas. For example, an altered gait in one leg may negatively affect the other leg over time, while an altered gait in both legs may negatively affect other

musculature.

8.3 Ethical Issues

Safety is a priority in our design. While it would be easier to design a device that was cheap and appeared functional in order to make a profit, that would be extremely unethical as it would cause injury to the user. This being considered, every factor of safety, every response time, and every limitation to our device is in itself, an ethical issue. The goal of the product, in every decision we have made and will make, must be to ensure the safety of the user, and to enable the user to function more normally in their day-to-day life.

If the device does experience mechanical or electrical failure, or the code malfunctions, it must do so in a manner that harms the user the least. Any moving parts are not without risk, but the goal is to minimize this risk. Our design has no pinch points, so that in normal operation, it is nearly impossible to injure one's self via moving parts. However, there is still risk of shrapnel if a part were to shatter. Our current product is only a proof of concept, but as we move forward, we will analyze the fracture mechanics of our chosen materials and determine what loads each part will experience. Each part should have a satisfactory factor of safety, and should have ductile failure if at all possible, so that failure is easy to detect and is not catastrophic.

There are a few other ethical issues in our design, although they are not as critical. Both the cost of the device, and the limitations it imposes on the user should be considered. If the cost is too high, it may become prohibitive, and prevent the people who need it the most from being able to afford it. Ideally, this could be resolved if we can get the device covered by the user's medical insurance. The limited mobility caused by the device could affect the user negatively, as explained in the Risk and Liability section. While that risk is an ethical issue much like safety, it is significantly harder to deal with and is an issue with current AFOs as well. Users should be given medically accurate warnings in order to deal with this. It is also noteworthy that the device provides increased mobility and independence, which outweighs the risks in many peoples' minds, and arguably remedies the ethical issues caused by the limited motion allowed by the device.

8.4 Impact on Society

While the prevalence of foot drop has not been quantified, it is a common condition that can limit the mobility and lifestyle of those affected [6]. Therefore, the successful development of our AFO will allow individuals who experience foot drop to move more independently. Our device may also allow individuals to move without the need for mobility aids, such as a wheelchair, or surgical procedures. There is then the potential to reduce the risks and costs associated with corrective surgical procedures and treatment for pain and injuries due to ankle hyperextension. We also believe that improving one's mobility will improve their health, well-being, and productivity. Slight pain when traveling or exercising can quickly and easily be alleviated, allowing users to focus more on themselves or their tasks.

8.5 Impact on the Environment

This device currently uses various plastics and metals, as well as a power supply and microcontroller. The final product will likely contain plastics and composite materials, as well as metal, and will use a smaller microcontroller and batteries. The production and eventual degradation of plastics and batteries both contribute to carbon emissions and can create other issues during the degradation process. The batteries must be disposed of properly when they eventually go bad, but as a society we are moving towards safer and less toxic batteries. Plastics and composites will likely be used in higher quantities than in the current product created by Fabtech Systems, but the volume of each of these materials is still relatively small and the increase in the users' quality of life will be massive. It is also noteworthy that many of the users of this product may otherwise be wheelchair-bound, and the environmental impact of a motorized wheelchair is far greater than that of our design.

It should also be mentioned that the user base for this product is quite small, meaning there will not be

many of them made, resulting in a low environmental impact overall.

8.6 Cost and Engineering Economics

The fabrication of this prototype cost approximately $700 (the cost of each component is broken down in Appendix E). For comparison, a single composite beam for the existing Fabtech beams costs about $230. However, because this design varies stiffness automatically, the user would only need one composite beam instead of five.

There are also some areas of potential cost reduction as this design is pushed to commercial production. The motor, amplifier, and power source that were used in the prototype design were much more powerful than would be necessary in the real product. For this reason, the commercial device can be designed with much more economical components and still perform the same function. It should also be noted that $220 of our fabrication costs went towards 3D printing. Many of these plastic parts are specific to the bench-top prototype, and would not be present in the commercial version. Additionally, all essential plastic components could be injection molded to save cost.

As noted earlier, this device has a relatively small target market, meaning that economies of scale will not have a large effect when this device comes to market. While this device would be significantly more expensive than the existing Fabtech system, it should be noted that because it is a medical device, it can be paid for by insurance. This means that the higher cost could be an acceptable trade off for convenience.

8.7 Codes and Standards

Most existing AFOs do not contain powered components and are therefore classified as a "Limb Orthosis" specified under Sec. 890.3475 in subpart D – Physical Medicine Prosthetic Devices of the FDA's Department of Health and Human Services Subchapter H – Medical Devices [7] Under this section, the orthotic is defined as a class 1 medical device and would adhere to general controls, but would be exempt from manufacturing practice requirements.

However, our device will use powered components and will therefore be classified as a "Powered Lower Extremity Exoskeleton" specified under Sec. 890.3480 in Subpart D – Physical Medicine Prosthetic devices. Our AFO would then be defined as a class II medical device, making our commercialization pathway more complicated. The special controls for this classification are:

1. Material biocompatibility
2. Safety and performance validation
3. Software verification
4. Consistency with intended use
5. Non-clinical performance testing
6. Clinical testing
7. Training program
8. Labeling

In bringing our device to market, we must then ensure that our materials are biocompatible with our intended patient. We must perform testing and analysis to ensure that every component is working as intended and the device is safe in electromagnetic, electrical, thermal, and mechanical aspects. Software and design composition must also be verified before demonstrating intended and safe performance in non-clinical and clinical trials. A training program for clinicians and users must then be developed to ensure that those involved are able to correctly operate the device and access all safety features. Labeling will require information regarding instructions, warnings, cautions, limitations, and safeguards.

9. Next steps

After the completion of this prototype, the next step is create a prototype that would attach to the pre-existing Fabtech System's AFO. This process would include changing the mechanical hardware to mount to their device. Along with that, a new cantilever beam would have to be developed such that it could withstand the forces and stiffnesses needed in a real world case scenario. Most likely this beam would have to be a carbon fiber composite beam which is able to support exponentially higher loads and stiffnesses.

For the software side of the design, a large change would be to only have the device change positions when the foot is in the air. The reason behind this is due to the fact that when the foot is on the ground, there are a lot more forces acting on the carriage which would require higher torques from the motor to move. This would demand more power from the system and more quickly drain out the battery. Another thing that would help combat the problem of power draw is increase the motor gearing. Obviously this would lower the speed of translation, but for this application, the speed does not need to be relatively high and this trade would be well worth it. Also a new motor would most likely be used which would have more specific characteristics for this exact device. Lastly, the device would want to include an amendment to the code that implements an averaging scheme of the past few steps so that the device is not as finicky. People do not change their pace frequently and this additional averaging of step angle would further lower the power draw of the entire system as it would adjust the position less often.

Finally, this new prototype that attaches to the Fabtech system would have to be tested on a human. This is most likely going to have unanticipated differences from the prototype made by us and will need to be fined tuned. This test would include analysis on the materials selected for the structure of the device, the cantilever beam, and the control system used to regulate the motion of the carriage to alter the effective length of the beam.

10. Conclusions

This project was a proof of concept for a variable stiffness beam that would be later used on an ankle - foot orthotic and would give many great insights on how such a device could operate. From the results, there were many promising features that showcase the effectiveness of this type of variable stiffness beam in a commercial device. This prototype showed the feasibility to control the translational motion of a carriage that would be responsible for changing the stiffness of a beam. From Figure 15, the capability of this design to accomplish the goal of changing the effective length automatically by simply analyzing the angle of the system as it is being used was confirmed. Also looking at Figure 16, it can be observed that even when the force was changed, the response in angle always migrated back to its set point of 5 degrees.

This prototype proves the control loop and all the algorithms are working as planned. It is simple enough to create a few CAD drawings of something that would be able to change stiffness mechanically. But then to introduce embedded computing into the mix adds another dimension of complexity. The results speak for themselves proving that the implementation of the embedded computing and the code behind it is capable of receiving data, analysing it, then creating a correct output to send back to the system.

This project also showed the feasibility of using 3D printed parts as the main structure of the device. There were a few doubts about the strength and rigidity of using 3D printed parts as the backbone of the device, but even with extensive analysis, each part is working well and has yet to show any signs of stress and damage. This could be very useful for the commercial product as 3D printing is significantly cheaper and faster to manufacture compared to composite or metal alternatives.

One other thing that should be quickly addressed is the team that worked on this project. We all showed an incredible amount of teamwork and problem solving skills throughout the duration of the project. One factor that did a lot in this accomplishment was that each member was obviously very passionate about this project and held the desire to make a working prototype. Due to the circumstances faced in the last quarter, it would have been easy to downscale the deliverable as still pass the class. Instead, everyone kept working hard and ended up making a very impressive device that hopefully will continue on and reach its full potential and really help some people. We would be remorseful to leave out another incredible factor and arguably the most important, our professor who helped and guided us the entire way, Dr. Joseph Garbini. Thank you!

References

[1] Skaaret, I., Steen, H., Huse, A. and Holm, I., 2019. Comparison of Gait With and Without Ankle-foot Orthoses after Lower Limb Surgery in Children with Unilateral Cerebral Palsy. *Journal of Children's Orthopaedics*, 13(2), pp.180-189..

[2] Kelly, B., 2009. AAOS Atlas of Orthoses and Assistive Devices. *JAMA*, 301(24), p.2596

[3] Budynas, R., Nisbett, J. and Shigley, J., 2015. *Shigley's Mechanical Engineering Design*.

[4] Physiopedia. 2020. Running Biomechanics. [online] Available at: <https://www.physiopedia.com/Running_\ Biomechanics> [Accessed 11 June 2020].

[5] Russell Esposito, E., Blanck, R., Harper, N., Hsu, J. and Wilken, J., 2014. How Does Ankle-foot Orthosis Stiffness Affect Gait in Patients With Lower Limb Salvage?. *Clinical Orthopaedics and Related Research*, 472(10), pp.3026-3035.

[6] Carolus, A., Becker, M., Cuny, J., Smektala, R., Schmieder, K. and Brenke, C., 2019. The interdisciplinary management of foot drop. *Deutsches Aerzteblatt Online*.

[7] FDA. (April 1, 2019) Medical Devices Part 890: Physical Medicine Devices Subpart D – Physical Medicine Prosthetic Devices. [Online].

Appendices

All of the appendix can be found in the parent folder that houses this document in a sub folder named Appendix.

Appendix A shows all of the mechanical references used in the report and project. This includes the two CAD models, both motor spec sheets, and the spec sheet for the FUYU linear rail lead screw

Appendix B shows all of the electrical references used in the report and the project. This includes the complete wiring diagram, and the spec sheets for the myRio, encoder, and amplifier. Appendix C shows all of the Eclipse C code that was used for this prototype including the primary main.C file as well as all of the included headers used in it.

Appendix D has all of the MATLAB and SIMULINK code files that were used in the analysis for this project as well as the creation of the controller constants.

Appendix E has a description of all the material purchased for this project as well as the final cost.

Appendix F has all of the media that was captured during the duration of the project.